Supporting Information for

Color tuning in red/green cyanobacteriochrome AnPixJ: Photoisomerization at C15 causes an excited-state destabilization

Chen Song,[1,2] Rei Narikawa,[3,4,5] Masahiko Ikeuchi,[4,6]

Wolfgang Gärtner,[7] and Jörg Matysik[1,2,*]

[1]*Leids Instituut voor Chemisch Onderzoek, Universiteit Leiden, P.O. Box 9502, 2300 RA Leiden, The Netherlands;*

[2]*Institut für Analytische Chemie, Universität Leipzig, Johannisallee 29, D-04103 Leipzig, Germany;*

[3]*Department of Biological Science, Faculty of Science, Shizuoka University, Ohya, Suruga-ku, Shizuoka 422-8529, Japan;*

[4]*Graduate School of Art and Sciences, University of Tokyo, Komaba, Meguro, Tokyo 153-8902, Japan;*

[5]*Precursory Research for Embryonic Science and Technology, Japan Science and Technology Agency, 4-1-8 Honcho Kawaguchi, Saitama 332-0012, Japan;*

[6]*Core Research for Evolutional Science and Technology, Japan Science and Technology Agency, 4-1-8 Honcho Kawaguchi, Saitama 332-0012, Japan;*

[7]*Max-Planck-Institut für Chemische Energiekonversion, Stiftstraße 34–36, D-45470, Mülheim an der Ruhr, Germany.*

*To whom correspondence should be addressed. E-mail: joerg.matysik@uni-leipzig.de.

This PDF file includes:

Supporting Information Text

Peak assignments of 1D ^{13}C CP/MAS NMR spectra of *u*-[^{13}C,^{15}N]-PCB-AnPixJg2 as Pr and Pg.

In the present study, ^{13}C CP/MAS spectrum of AnPixJg2 display far-reaching similarities with that for Cph1Δ2 in the red-absorbing 15*Z* dark state (Figure 2). The complete ^{13}C assignment for Cph1Δ2 as Pr (for review *see* ref. 1) thus forms the basis for assignment of the corresponding AnPixJg2 peaks (summarized in Table S1). The revealed Pr similarity in overall structure of AnPixJg2[2] and Cph1-GAF,[3] particularly in view of the chromophore geometry and its immediate protein environment facilitates our interpretation of the AnPixJg2 data. However, an unambiguous assignment is not possible at current stage of research since the low amount of protein used (~1.3 mg) and the poor chromophore incorporation ratio precludes observation of well-resolved spectral lines in a 2D mode.

^{13}C Pr spectra of AnPixJg2 (red) and Cph1Δ2 Pr (purple) are shown in Figure 2. The spectral region of 85–115 ppm contains three methine bridge carbons (C5, C10, and C15, for numbering *see* Figure 2, *Inset*). In Cph1Δ2 C5, C10, and C15 locate at $\delta^C = 87.1$, 112.8, and 93.2 ppm, respectively, whereas in AnPixJg2, three well-separated signals are observed at $\delta^C = 85.4$, 114.4, and 97.0 ppm. We first note that the signal at 85.4 ppm can be unambiguously identified as C5 by virtue of its distinct upfield ^{13}C chemical shift among those three carbons seen in the form of free PCB,[4] and also after assembly with the cyanobacterial and plant phytochromes.[5,6] In both Pr structures of AnPixJg2 (3W2Z) and Cph1 (2VEA), rings ***B***–***C*** adopt a nearly identical coplanar conformation (Figure 2, *Inset*) giving a strong hint that the C10 response in AnPixJg2 would resonate closely to that of Cph1Δ2 ($\delta^C = 112.8$ ppm). Therefore, we assign the signal at $\delta^C = 114.4$ ppm (red) to C10, with a $\Delta\delta^C$ of 1.6 ppm to that of Cph1Δ2. The remaining signal in this region ($\delta^C = 97.0$ ppm) can be directly assigned to C15 with a relatively large $\Delta\delta^C$ of +3.8 ppm between the two C15 responses.

The much larger distortion angle of ring ***D*** relative to the coplanar ***B***–***C*** plain in AnPixJg2 (60.8°) than in Cph1 (26.3°) might be the origin of the observed $\Delta\delta^{C15}$. Pyrrolic quaternary carbons lie between 120 and 155 ppm, including C6–C9 and C11–C14 of the two inner rings ***B*** and ***C*** as well as C4 and C16–C18 of the two terminal pyrrolenine rings ***A*** and ***D***. In the case of AnPixJg2, twelve simulated chromophore peaks have been determined at δ^{C} of 150.8, 147.9, 147.1, 145.4, 144.2, 143.1, 141.2, 132.0, 128.1, 126.7, 125.7, and 122.8 ppm. For two C5 peaks as Pr, a small $\Delta\delta^{C}$ is observed (1.7 ppm), the similarity should also be kept for its two carbon neighbors, hence the signals resonating at $\delta^{C} = 150.8$ and 147.9 ppm are tentatively assigned to C4 and C6, respectively. In such a case, their δ^{C} best match those of Cph1Δ2 ($\delta^{C4/C6} = 153.9/149.5$ ppm).

In Cph1Δ2 Pr, the chemical shifts of C8 and C9 of the ring ***B*** are mirror dual to C12 ($\delta^{C8/C12} = 127.7$ ppm) and C11 ($\delta^{C9/C11} = 145.2$ ppm) of the ring ***C*** on C10. Such mirror image is not duplicated by AnPixJg2 chromophore, although the signals of C9 and C11 ($|\Delta\delta^{C}| = 1.4$ ppm; $\delta^{C9/C11} = 126.7/128.1$ ppm) as well as C8 and C12 ($|\Delta\delta^{C}| = 1.1$ ppm; $\delta^{C8/C12} = 144.2/143.1$ ppm) resonate at very similar ^{13}C shifts. It is not possible to discriminate these two sets solely based on the comparison of the two Pr spectra shown in Figure 2. However, the relevant $\Delta\delta^{C}$ occurring during photoconversion to Pg (Dataset S1) makes an assignment of the upfield signal at 143.1 ppm to C12 more plausible (*see* below). Likewise, the signal at $\delta^{C} = 126.7$ ppm can be assigned to C9, and the peak sitting at 128.1 ppm is thus attributed to C11 (*see* below). Another set of two partially overlapped signals at $\delta^{C} =$ 147.1 and 145.4 ppm correspond to C14 and C16, the assignment would remain ambiguous, however, their distinction is not crucial for the following discussion. Two quaternary carbons resonating between C8/C12 and C9/C11 can be readily distinguished as C17 ($\delta^{C} = 141.2$ ppm) and C18 ($\delta^{C} = 132.0$ ppm) of the ring ***D***, since both are found at the slight up-field positions of the corresponding C17 and C18 peaks ($\delta^{C} = 142.1$ and 134.0 ppm, respectively) from Cph1Δ2. Similarly, we assigned the remaining AnPixJg2 signals at 122.8 and 125.7 ppm to C7 and C13,

respectively which differ by 2.9 and 0.7 ppm from the Cph1Δ2 counterparts (Table S1). In the region above 170 ppm, signals for carbonyl groups of both terminal rings and propionate carboxylate moieties of the two inner rings are found. The most intense signal at 174.0 ppm is most likely due to the ***D***-ring carbonyl (C19), especially in comparison with that of Cph1Δ2 at $\delta^{C} = 172.7$ ppm, these two peaks are of roughly equal intensity and differ by only 1.3 ppm. The high CP efficiency of this carbonyl in both cases would be probably due to their extensive hydrogen-bonding interactions with the binding pocket (*e.g.*, H290Nε2 in Cph1, ~2.8 Å *vs*. Y352Oη in AnPixJg2, ~2.6 Å, *see* Figure 1b), two carbonyl groups thus positioned in close proximity to a region with high proton density. The ***A***-ring carbonyl (C1) in AnPixJg2 can be easily identified as the most low-field signal at $\delta^{C} = 182.8$ ppm which is relatively upfield displaced by 1.2 ppm to that of Cph1Δ2 and becomes a non-resolved shoulder of a strong signal at ~180 ppm representing two carboxylates. In the red/green-type CBCRs, the ***A***-ring carbonyl (C1) is hydrogen-bonded to a unique Trp residue (Figure 1b), whereas no such strong interactions are found in Cph1Δ2 (Figure 1a). This might explain the observed peak enhancement of C1 in AnPixJg2. The unequivocal assignment of the two carboxylate peaks in AnPixJg2 ($\delta^{C} = 179.0/181.0$ ppm) is not yet available, however, it seems more likely that the signal at 179.0 ppm originates from $C12^{3}$, with identical δ^{C} to that of Cph1Δ2 (Table S1). The 12-propionates of ring ***C*** are suggested to be similarly orientated in 3W2Z and 2VEA (Figure 2, *Inset*). In contrast, the 8-propionate of ring ***B*** is rotationally twisted in 3W2Z. The expectation that the larger $\Delta\delta^{C}$ would be observed at the 8-propionate in fact match the assignment of $C8^{2}$ and $C12^{2}$ methylene carbons on the basis of comparison with Cph1Δ2, in which $\Delta\delta^{C}$ of $C8^{2}$ and $C12^{2}$ are of –1.5 and +0.5 ppm, respectively (Table S1).

The methylene signals occurring between 30 and 80 ppm arise from three ***A***-ring carbons, C2, C3, and $C3^{1}$. If we assume that the AnPixJg2 signal at $\delta^{C} = 50.8$ ppm corresponds to $C3^{1}$ of Cph1Δ2 ($\delta^{C} = 47.6$ ppm), $\Delta\delta^{C}$ for two $C3^{1}$ would be 3.2 ppm. The assumption is supported by the comparison of

3W2Z and 2VEA that implies the difference in electronic structure of two C3^1 atoms due to opposite stereochemistry at this position (Figure 2, *Inset*). However, the stereochemistry at C2 atom in both cases has been determined to be exclusively in *R*, the similar configuration is in accordance with the observed small $\Delta\delta^C$ between two C2 atoms ($|\Delta\delta^{C2}| = 1.4$ ppm with $\delta^{C2} = 35.7$ ppm in AnPixJg2). It should be noted that, in this region, the peak intensities of methylene groups show an overall increase in AnPixJg2. Similar peak enhancement is also seen in the spectral region below 30 ppm containing two methylene carbons of propionates at rings ***B*** and ***C*** (C8^1 and C12^1), the ***D***-ring ethyl group (C18^1 and C18^2) as well as the methyl groups of four rings. Comparison of the two Pr spectra also indicates that δ^C of all methyl and methylene sites are barely affected by the PCB-binding pocket ($\Delta\delta^C$ ranging from –1.3 to +1.4 ppm, Table S1).

In Figure 3a, the ^{13}C spectrum of AnPixJg2 as Pr (red) is superimposed with that as Pg (blue). As Pg, the signals resolved at $\delta^C = 85.9$ and 113.7 ppm correspond to C5 and C10, respectively, locating almost identical to those as Pr ($\delta^C = 85.4/114.4$ ppm). However, a larger $\Delta\delta^C$ (as Pg – Pr in the case of AnPixJg2) of +2.3 ppm is found to be associated with the C15-methine bridge between rings ***C*** and ***D***. Pg signals below 80 ppm representing methyl and methylene groups of the chromophore are mostly upfield shifted relative to those of Pr (Table S1), among which the largest $\Delta\delta^C$ arise from the two ethyl groups of the terminal rings, C3^1 ($\Delta\delta^C = +1.9$ ppm) of ring ***A*** as well as C18^2 of ring ***D*** ($\Delta\delta^C = +1.4$ ppm). Comparison of the two spectra reveals a prominent spectral change in the low-field region, referring to the ***D***-ring carbonyl (C19) which shifts upfield from 174.0 ppm as Pr to 168.9 ppm as Pg ($\Delta\delta^C = -5.1$ ppm). Such an assignment is strongly corroborated by the $\Delta\delta^{C19}$ of –3.6 ppm in Cph1Δ2 (Table S1) following an analogous $Z \rightarrow E$ isomerization around C15=C16 double bonds. In the ^{13}C liquid- and solid-state NMR spectra of the free PCB as monomer/dimer[4] and covalently bound to Cph1Δ2 and plant phytochromes,[5,6] the ***A***-ring carbonyl (C1) signals were consistently situated at most low-field position. Similarly, in both photostates of AnPixJg2, we

attribute the most deshielded peaks to C1 ($\delta^C = 184.4$ and 182.8 ppm as Pg and Pr, respectively). Also in this region, two remaining well-resolved Pg signals at $\delta^C = 181.2$ and 174.9 ppm can be assigned to the C8- and C12-carboxylate ($C8^3$ and $C12^3$), respectively, on the basis of the corresponding $\Delta\delta^C$ upon the Pr-to-Pfr photoconversion of Cph1Δ2 (Table S1). The most probable cause for the observed –4.1-ppm $\Delta\delta^C$ of $C12^3$ is a rearrangement of the hydrogen-bonding network around the ***C***-ring propionate side-chain upon Pg formation. For the ***B***-ring counterpart in AnPixJg2, its location is stabilized by the hydrogen bonds with the imidazoles of two His residues (H318 and H322, Figure 1b). The $C8^3$-response as Pg locating at 181.2 ppm remains unaffected ($\Delta\delta^C = +0.2$ ppm) suggesting that these two His residues may alter the conformations of their imidazoles in concert with the motion of the chromophore upon Pg formation, and thus maintain the local electrostatic and electronic environment of the carboxylate.

As Pr, the δ^C of the pyrrolic carbons are distributed over 18.8 ppm between 150.8 and 141.2 ppm as well as between 132.0 and 122.8 ppm, while as Pg, we observed a 28.2-ppm δ^C ranging from 152.9 to 137.0 ppm and from 131.9 to 119.6 ppm (Figure 2). The expanded δ^C range of the pyrrole carbons as Pg indicates that the Pr → Pg photoconversion presumably involves a charge redistribution around the chromophore. In comparison with Pr, two Pg signals resonating at $\delta^C = 152.9$ and 150.4 ppm can be attributed to the adjacent carbons of the methine bridge linking rings ***A*** and ***B*** (C4 and C6). Assuming that C4 of the ring ***A*** locates at more downfield position of 152.9 ppm (and thus C6 at 150.4 ppm), the light-induced $\Delta\delta^{C4}$ and $\Delta\delta^{C6}$ would be +2.1 and +2.5 ppm, respectively, inconsistent with the subtle $\Delta\delta^{C5}$ of +0.2 ppm. Hence, the above assumption seems not valid and the assignment of these two carbons should be reversed, that is, $\delta^{C4/C6} = 150.4/152.9$ ppm with the corresponding $\Delta\delta^{C4}$ and $\Delta\delta^{C6}$ of –0.2 and +5.0 ppm, respectively. In a similar manner, the assignment of the adjacent carbons of C10 is obtained: C11 of ring ***C*** resonates at $\delta^C = 127.3$ ppm, corresponding to a $\Delta\delta^C$ of –0.8 ppm, whereas C9 of ring ***B*** is detected at $\delta^C = 131.9$ ppm with a $\Delta\delta^C$

of +5.2 ppm. Such dramatic shifts of C6 and C9 are directly related to the deprotonation of the ***B***-ring pyrrole nitrogen.[4] Further, the signals at $\delta^C = 122.1$ and 119.6 ppm would come from C7 and C13, respectively. This assignment is achieved from the characteristic $\Delta\delta^C$ pattern for C7 and C13 in Cph1Δ2 associated with an analogous C15-*Z*/*E* photoisomerization ($\Delta\delta^{C7/C13} = +0.4/+4.3$ ppm); however, it should be noted that the $\Delta\delta^{C13}$ in AnPixJg2 Pr→Pg shows an opposite sign (–6.1 ppm). For the $\Delta\delta^C$ of three pyrrolic carbons of ring ***B*** (C6, C7, and C9) between Pr and Pg, their overall trend and signs are opposite to those in the N22 protonation during assembly of PCB into Cph1Δ2 apoprotein.[4] $\Delta\delta^{C8}$ can be reasonably expected to correlate with the $\Delta\delta^C$ of other ***B***-ring carbons, hence the signal at $\delta^C = 143.6$ ppm was assigned to C8 with a $\Delta\delta^C$ of –0.6 ppm ($\Delta\delta^{C8} = +2.4$ ppm upon PCB assembly, ref. 4). Five unassigned pyrrole peaks as Pg at $\delta^C = 145.9$, 139.7, 138.7, 137.0, and 141.3 ppm result from C12, C14, C16, C17, and C18, among which the signal at $\delta^C = 145.9$ ppm can be only attributed to C17, considering the $\Delta\delta^C$ with the corresponding Pr peaks of above unassigned Pg ones at 143.1, 147.1, 145.4, 141.2, and 132.0 ppm. Besides a $\Delta\delta^C$ of +4.7 ppm with the C17 as Pr at 141.2 ppm, other $\Delta\delta^C$ appear to be either too small (*e.g.*, +2.8, –1.2, and +0.5 ppm with $\delta^C = 143.1$, 147.1, and 145.4 ppm, respectively) or too large (*e.g.*, +13.9 ppm with $\delta^C = 132.0$ ppm) to correlate with the C15-isomerization seen in Cph1Δ2 (Table S1) and the $\Delta\delta^C$ observed for the other ***D***-ring carbons in AnPixJg2 (*see* below). For C12, however, the change in bilin protonation state is likely to play a more prominent role than photoisomerization in tuning the δ^C: $\Delta\delta^{C12}$ was found to be –14.7 and +0.6 ppm upon assembly of PCB into Cph1Δ2 apoprotein[4] and Pfr formation in Cph1Δ2 (Table S1), respectively. It therefore seems to be most plausible to assign the Pg signal at 138.7 ppm to C12 since the resulting $\Delta\delta^C$ of –4.4 ppm would be most correlated to the $\Delta\delta^C$ for C6 and C9 induced by N22 deprotonation (*see* above). It should be noted that no evidence allows a one-to-one assignment of three remaining Pg signals at $\delta^C = 139.7$, 137.0, and 141.3 ppm for C14, C16, and C18; however, in any case, the Pr signals of C14 and C16 ($\delta^C = 147.1$ and 145.4

ppm) will exhibit large upfield shifts (> 4.1 ppm) during photoconversion, whereas the C18 Pr signal at 132.0 ppm will be displaced downfield by at least 5.0 ppm (Table S1).

References

1. Song, C.; Rohmer, T.; Tiersch, M.; Zaanen, J.; Hughes, J.; Matysik, J. *Photochem. Photobiol.* **2013**, *89*, 259–273.
2. Narikawa, R.; Ishizuka, T.; Muraki, N.; Shiba, T.; Kurisu, G.; Ikeuchi, M. *Proc. Natl. Acad. Sci. U.S.A.* **2013**, *110*, 918–923.
3. Essen, L.-O.; Mailliet, J.; Hughes, J. *Proc. Natl. Acad. Sci. U.S.A.* **2008**, *105*, 14709–14714.
4. Rohmer, T.; Lang, C.; Gärtner, W.; Hughes, J.; Matysik, J. *Photochem. Photobiol.* **2010**, *86*, 856–861.
5. Song, C.; Psakis, G.; Lang, C.; Mailliet, J.; Gärtner, W.; Hughes, J.; Matysik, J. *Proc. Natl. Acad. Sci. U.S.A.* **2011**, *108*, 3842–3847.
6. Song, C.; Essen, L.-O.; Gärtner, W.; Hughes, J.; Matysik, J. *Mol Plant* **2012**, *5*, 698–715.
7. Rockwell, N. C.; Martin, S. S.; Lim, S.; Lagarias, J. C.; Ames, J. B. *Biochemistry* **2015**, *54*, 2581–2600.

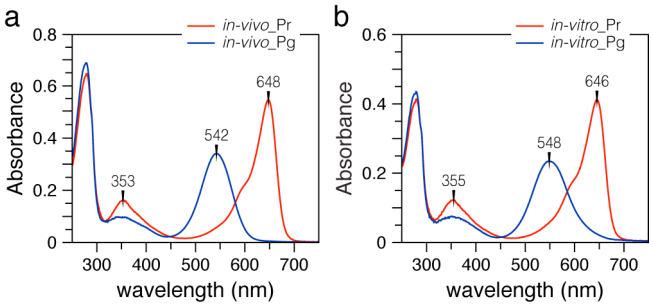

Figure S1. *In-vivo* and *in-vitro* assembly of [$^{15}N_4$]-PCB with AnPixJg2. Electronic absorption spectra of AnPixJg2 generated by *in-vivo* (a) and *in-vitro* (b) assembly in the Pr (red) and Pg photoproduct (blue) states. Spectra of the Pr and Pg were obtained following irradiation at 530 and 660 nm light, respectively.

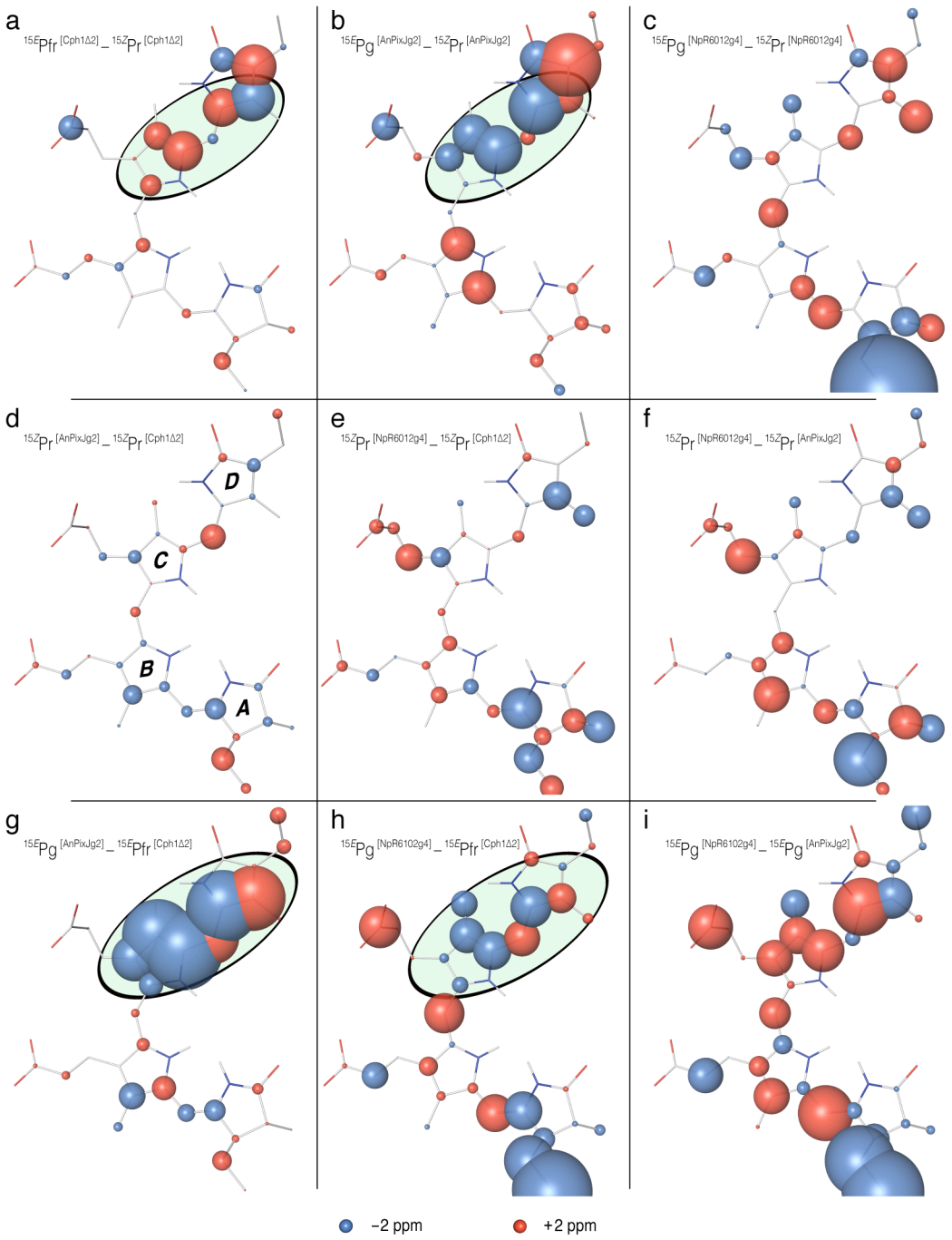

Figure S2 Schematic of $\Delta\delta^C$ of PCB chromophore accompanying 15*Z*-to-15*E* isomerization in two red/green-type CBCRs of AnPixJg2 and NpR6102g4 and in cyanobacterial phytochrome Cph1Δ2 as well as $\Delta\delta^C$ among the 15*Z* dark states and 15*E* photoproducts. All $\Delta\delta^C$ illustrated in panels are taken from Table S2. (a–c) $\Delta\delta^C$ accompanying 15*Z*-to-15*E* isomerization (as 15*E* – 15*Z*) in three photoreceptors of Cph1Δ2 (a), AnPixJg2 (b), and NpR6102g4 (c). (d–f) $\Delta\delta^C$ among the three 15*Z* Pr states: AnPixJg2 *vs*. Cph1Δ2 (as AnPixJg2 – Cph1Δ2, c), NpR6102g4 *vs*. Cph1Δ2 (as NpR6102g4 – Cph1Δ2, d), and NpR6102g4 *vs*. AnPixJg2 (as NpR6102g4 – AnPixJg2, e). (g–i) $\Delta\delta^C$ among the three 15*E* photoproducts: AnPixJg2 Pg *vs*. Cph1Δ2 Pfr (as AnPixJg2 Pg – Cph1Δ2 Pfr, g), NpR6102g4 Pg *vs*. Cph1Δ2 Pfr (as NpR6102g4 Pg – Cph1Δ2 Pfr, h), and NpR6102g4 Pg *vs*. AnPixJg2 Pg (as NpR6102g4 Pg – AnPixJg2 Pg, i). Carbons and nitrogens are colored gray and blue, respectively. The red and blue spheres represent down- and upfield shifts, respectively.

chromophore carbon		*u*-[^{13}C,^{15}N]-PCB-Cph1Δ2[§]			*u*-[^{13}C,^{15}N]-PCB-AnPixJg2[‡]			AnPixJg2 – Cph1Δ2	
		^{15Z}Pr	^{15E}Pfr	^{15E}Pfr – ^{15Z}Pr	^{15Z}Pr	^{15E}Pg	^{15E}Pg – ^{15Z}Pr	^{15Z}Pr – ^{15Z}Pr	^{15E}Pg – ^{15E}Pfr
	1	184.0	182.8	**−1.2**	182.8	184.4	**+1.6**	**−1.2**	**+1.6**
	2	37.1	37.2	**+0.1**	35.7	37.7	**+2.0**	**−1.4**	**+0.5**
	2^{1}	17.5	18.5	**+1.0**	16.9	18.2	**+1.3**	**−0.6**	**−0.3**
ring A	**3**	53.4	54.3	**+0.9**	54.5	55.4	**+0.9**	**+1.1**	**+1.1**
	3^{1}	47.6	50.0	**+2.4**	50.8	52.7	**+1.9**	**+3.2**	**+2.7**
	3^{2}	21.8	21.4	**−0.4**	23.2	21.7	**−1.5**	**+1.4**	**+0.3**
	4	153.9	153.5	**−0.4**	150.8	150.4	**−0.4**	**−3.1**	**−3.1**
A–B	**5**	87.1	88.5	**+1.4**	85.4	85.9	**+0.5**	**−1.7**	**−2.6**
	6	149.5	149.3	**−0.2**	147.9	152.9	**+5.0**	**−1.6**	**+3.6**
	7	125.7	126.1	**+0.4**	122.8	122.1	**−0.7**	**−2.9**	**−4.0**
	7^{1}	9.2	9.3	**+0.1**	8.7	7.9	**−0.8**	**−0.5**	**−1.4**
ring B	**8**	145.2	143.8	**−1.4**	144.2	143.6	**−0.6**	**−1.0**	**−0.2**
	8^{1}	21.8	23.1	**+1.3**	22.3	23.1	**+0.8**	**+0.5**	**0.0**
	8^{2}	42.9	41.8	**−1.1**	41.4	43.1	**+1.7**	**−1.5**	**+1.3**
	8^{3}	180.0	180.5	**+0.5**	181.0	181.2	**+0.2**	**+1.0**	**+0.7**
	9	127.7	129.9	**+2.2**	126.7	131.9	**+5.2**	**−1.0**	**+2.0**
B–C	**10**	112.8	112.4	**−0.4**	114.4	113.7	**−0.7**	**+1.6**	**+1.3**
	11	127.7	131.0	**+3.3**	128.1	127.3	**−0.8**	**+0.4**	**−3.7**
	12	145.2	145.8	**+0.6**	143.1	138.7	**−4.4**	**−2.1**	**−7.1**
	12^{1}	20.4	20.5	**+0.1**	19.1	20.4	**+1.3**	**−1.3**	**−0.1**
ring C	**12^{2}**	38.1	38.4	**+0.3**	38.6	38.8	**+0.2**	**+0.5**	**+0.4**
	12^{3}	179.0	175.3	**−3.7**	179.0	174.9	**−4.1**	**0.0**	**−0.4**
	13	126.4	130.7	**+4.3**	125.7	119.6	**−6.1**	**−0.7**	**−11.1**
	13^{1}	11.4	11.6	**+0.2**	12.2	11.9	**−0.3**	**+0.8**	**+0.3**
	14	145.9	152.0	**+6.1**	147.1	139.7	**−7.4**	**+1.2**	**−12.3**
C–D	**15**	93.2	91.6	**−1.6**	97.0	99.3	**+2.3**	**+3.8**	**+7.7**
	16	145.9	151.6	**+5.7**	145.4	137.0	**−8.4**	**−0.5**	**−14.6**
	17	142.1	135.5	**−6.6**	141.2	145.9	**+4.7**	**−0.9**	**+10.4**
	17^{1}	9.9	10.0	**+0.1**	10.1	10.5	**+0.4**	**+0.2**	**+0.5**
ring D	**18**	134.0	140.5	**+6.5**	132.0	141.3	**+9.3**	**−2.0**	**+0.8**
	18^{1}	16.5	15.6	**−0.9**	16.2	17.7	**+1.5**	**−0.3**	**+2.1**
	18^{2}	13.2	13.3	**+0.1**	14.6	15.6	**+1.0**	**+1.4**	**+2.3**
	19	172.7	169.1	**−3.6**	174.0	168.9	**−5.1**	**+1.3**	**−0.2**

[§]The assignments of *u*-[^{13}C,^{15}N]-PCB-Cph1Δ2 in both photostates were done on the basis of Supporting Information ref. 1.

[‡]The assignments of C14 and C16 (single underlined) of *u*-[^{13}C,^{15}N]-PCB-AnPixJg2 in the 15*Z* state could be interchanged. Similarly, as the green-absorbing 15*E* photoproduct, the assignments of C14, C16, and C18 (double underlined) are not conclusive. Detailed assignments for both photostates were given in the main text.

Table S1 Overview of ^{13}C chemical shifts of PCB (δ^{C}) upon assembly into Cph1Δ2 and AnPixJg2. The data were obtained from holoproteins of Cph1Δ2 and AnPixJg2 generated by *in vitro* assembly with uniformly ^{13}C- and ^{15}N-labeled PCB chromophore (*u*-[^{13}C, ^{15}N]-PCB-Cph1Δ2 and *u*-[^{13}C, ^{15}N]-PCB-AnPixJg2, respectively). Both *in vitro* assembled holoproteins were measured in the respective 15*Z* (Pr) and 15*E* (Pfr for Cph1Δ2, and Pg for AnPixJg2) photostates. $\Delta\delta^{C}$ between the red-absorbing 15*Z* dark state and far-red-absorbing 15*E* photoproduct of Cph1Δ2 (^{15E}Pfr – ^{15Z}Pr), $\Delta\delta^{C}$ between the red-absorbing 15*Z* state and green-absorbing 15*E* photoproduct of AnPixJg2 (^{15E}Pg – ^{15Z}Pr), $\Delta\delta^{C}$ between two 15*Z* red-absorbing dark states (^{15Z}Pr – ^{15Z}Pr as AnPixJg2 – Cph1Δ2), and $\Delta\delta^{C}$ between two 15*E* photoproducts (^{15E}Pg – ^{15E}Pfr as AnPixJg2 – Cph1Δ2) were listed and illustrated in Figure 4.

		Cph1Δ2[§]			AnPixJg2[†]			NpR6012g4[‡]			AnPixJg2 – Cph1Δ2		NpR6012g4 – Cph1Δ2		NpR6012g4 – AnPixJg2	
chromophore	carbon	^{15Z}Pr	^{15E}Pfr	^{15E}Pfr – ^{15Z}Pr	^{15Z}Pr	^{15E}Pg	^{15E}Pg – ^{15Z}Pr	^{15Z}Pr	^{15E}Pg	^{15E}Pg – ^{15Z}Pr	^{15Z}Pr – ^{15Z}Pr	^{15E}Pg – ^{15E}Pfr	^{15Z}Pr – ^{15Z}Pr	^{15E}Pg – ^{15E}Pfr	^{15Z}Pr – ^{15Z}Pr	^{15E}Pg – ^{15E}Pg
	1	184.0	182.8	**−1.2**	182.8	184.4	**+1.6**	183.3	183.6	**+0.3**	**−1.2**	**+1.6**	**−0.7**	**+0.8**	**+0.5**	**−0.8**
	2	37.1	37.2	**+0.1**	35.7	37.7	**+2.0**	40.5	36.4	**−4.1**	**−1.4**	**+0.5**	**+3.4**	**−0.8**	**+4.8**	**−1.3**
	2[1]	17.5	18.5	**+1.0**	16.9	18.2	**+1.3**	12.9	16.9	**+4.0**	**−0.6**	**−0.3**	**−4.6**	**−1.6**	**−4.0**	**−1.3**
ring A	**3**	53.4	54.3	**+0.9**	54.5	55.4	**0.9**	55.9	51.1	**−4.8**	**+1.1**	**+1.1**	**+2.5**	**−3.2**	**+1.4**	**−4.3**
	3[1]	47.6	50.0	**+2.4**	50.8	52.7	**+1.9**	43.5	43.0	**−0.5**	**+3.2**	**+2.7**	**−4.1**	**−7.0**	**−7.3**	**−9.7**
	3[2]	21.8	21.4	**−0.4**	23.2	21.7	**−1.5**	25.0	10.6	**−14.4**	**+1.4**	**+0.3**	**+3.2**	**−10.8**	**+1.8**	**−11.1**
	4	153.9	153.5	**−0.4**	150.8	150.4	**−0.4**	148.0	148.0	**0.0**	**−3.1**	**−3.1**	**−5.9**	**−5.5**	**−2.8**	**−2.4**
A–B	**5**	87.1	88.5	**+1.4**	85.4	85.9	**+0.5**	89.0	94.0	**+5.0**	**−1.7**	**−2.6**	**+1.9**	**+5.5**	**+3.6**	**+8.1**
	6	149.5	149.3	**−0.2**	147.9	152.9	**+5.0**	147.2	150.9	**+3.7**	**−1.6**	**+3.6**	**−2.3**	**+1.6**	**−0.7**	**−2.0**
	7	125.7	126.1	**+0.4**	122.8	122.1	**−0.7**	128.2	127.5	**−0.7**	**−2.9**	**−4.0**	**+2.5**	**+1.4**	**+5.4**	**+5.4**
	7[1]	9.2	9.3	**+0.1**	8.7	7.9	**−0.8**	9.0	8.5	**−0.5**	**−0.5**	**−1.4**	**−0.2**	**−0.8**	**+0.3**	**+0.6**
ring B	**8**	145.2	143.8	**−1.4**	144.2	143.6	**−0.6**	146.5	146.7	**+0.2**	**−1.0**	**−0.2**	**+1.3**	**+2.9**	**+2.3**	**+3.1**
	8[1]	21.8	23.1	**+1.3**	22.3	23.1	**+0.8**	21.3	22.8	**+1.5**	**+0.5**	**0.0**	**−0.5**	**−0.3**	**−1.0**	**−0.3**
	8[2]	42.9	41.8	**−1.1**	41.4	43.1	**+1.7**	41.0	37.8	**−3.2**	**−1.5**	**+1.3**	**−1.9**	**−4.0**	**−0.4**	**−5.3**
	8[3]	180.0	180.5	**+0.5**	181.0	181.2	**+0.2**	181.7	181.3	**−0.4**	**+1.0**	**+0.7**	**+1.7**	**+0.8**	**+0.7**	**+0.1**
	9	127.7	129.9	**+2.2**	126.7	131.9	**+5.2**	130.0	129.0	**−1.0**	**−1.0**	**+2.0**	**+2.3**	**−0.9**	**+3.3**	**−2.9**
B–C	**10**	112.8	112.4	**−0.4**	114.4	113.7	**−0.7**	114.0	118.5	**+4.5**	**+1.6**	**+1.3**	**+1.2**	**+6.1**	**−0.4**	**+4.8**
	11	127.7	131.0	**+3.3**	128.1	127.3	**−0.8**	128.3	128.5	**+0.2**	**+0.4**	**−3.7**	**+0.6**	**−2.5**	**+0.2**	**+1.2**
	12	145.2	145.8	**+0.6**	143.1	138.7	**−4.4**	142.1	144.3	**+2.2**	**−2.1**	**−7.1**	**−3.1**	**−1.5**	**−1.0**	**+5.6**
	12[1]	20.4	20.5	**+0.1**	19.1	20.4	**+1.3**	24.6	21.1	**−3.5**	**−1.3**	**−0.1**	**+4.2**	**+0.6**	**+5.5**	**+0.7**
ring C	**12[2]**	38.1	38.4	**+0.3**	38.6	38.8	**+0.2**	40.0	38.3	**−1.7**	**+0.5**	**+0.4**	**+1.9**	**−0.1**	**+1.4**	**−0.5**
	12[3]	179.0	175.3	**−3.7**	179.0	174.9	**−4.1**	181.2	181.5	**+0.3**	**0.0**	**−0.4**	**+2.2**	**+6.2**	**+2.2**	**+6.6**
	13	126.4	130.7	**+4.3**	125.7	119.6	**−6.1**	127.2	125.3	**−1.9**	**−0.7**	**−11.1**	**+0.8**	**−5.4**	**+1.5**	**+5.7**
	13[1]	11.4	11.6	**+0.2**	12.2	11.9	**−0.3**	10.4	7.5	**−2.9**	**+0.8**	**+0.3**	**−1.0**	**−4.1**	**−1.8**	**−4.4**
	14	145.9	152.0	**+6.1**	147.1	139.7	**−7.4**	146.3	146.2	**−0.1**	**+1.2**	**−12.3**	**+0.4**	**−5.8**	**−0.8**	**+6.5**
C–D	**15**	93.2	91.6	**−1.6**	97.0	99.3	**+2.3**	95.0	97.0	**+2.0**	**+3.8**	**+7.7**	**+1.8**	**+5.4**	**−2.0**	**−2.3**
	16	145.9	151.6	**+5.7**	145.4	137.0	**−8.4**	145.2	145.5	**+0.3**	**−0.5**	**−14.6**	**−0.7**	**−6.1**	**−0.2**	**+8.5**
	17	142.1	135.5	**−6.6**	141.2	145.9	**+4.7**	137.9	139.9	**+2.0**	**−0.9**	**+10.4**	**−4.2**	**+4.4**	**−3.3**	**−6.0**
	17[1]	9.9	10.0	**+0.1**	10.1	10.5	**+0.4**	6.7	11.6	**+4.9**	**+0.2**	**+0.5**	**−3.2**	**+1.6**	**−3.4**	**+1.1**
ring D	**18**	134.0	140.5	**+6.5**	132.0	141.3	**+9.3**	134.3	139.3	**+5.0**	**−2.0**	**+0.8**	**+0.3**	**−1.2**	**+2.3**	**−2.0**
	18[1]	16.5	15.6	**−0.9**	16.2	17.7	**+1.5**	17.2	16.6	**−0.6**	**−0.3**	**+2.1**	**+0.7**	**+1.0**	**+1.0**	**−1.1**
	18[2]	13.2	13.3	**+0.1**	14.6	15.6	**+1.0**	13.0	11.5	**−1.5**	**+1.4**	**+2.3**	**−0.2**	**−1.8**	**−1.6**	**−4.1**
	19	172.7	169.1	**−3.6**	174.0	168.9	**−5.1**	174.0	171.3	**−2.7**	**+1.3**	**−0.2**	**+1.3**	**+2.2**	**0.0**	**+2.4**

[§]Supporting Information ref. 1; [†]current work; [‡]SI ref. 7.

Table S2 Overview of ^{13}C chemical shifts (δ^C) of PCB in Cph1Δ2 phytochrome and two red/green CBCRs AnPixJg2 and NpR6102g4. $\Delta\delta^C$ of PCB chromophore accompanying 15*Z*-to-15*E* isomerization in the three photosensors as well as $\Delta\delta^C$ among their 15*Z* dark states and 15*E* photoproducts were listed and illustrated in Figure S2.